ESTCP
Cost and Performance Report

(MR-200603)

MetalMapper: A Multi-Sensor TEM System for UXO Detection and Classification

April 2011

ESTCP

ENVIRONMENTAL SECURITY
TECHNOLOGY CERTIFICATION PROGRAM

U.S. Department of Defense

Report Documentation Page

Form Approved
OMB No. 0704-0188

1. REPORT DATE	2. REPORT TYPE	3. DATES COVERED
APR 2011	**N/A**	**-**

4. TITLE AND SUBTITLE	5a. CONTRACT NUMBER
MetalMapper: A Multi-Sensor TEM System for UXO Detection and Classification	5b. GRANT NUMBER
	5c. PROGRAM ELEMENT NUMBER
6. AUTHOR(S)	5d. PROJECT NUMBER
	5e. TASK NUMBER
	5f. WORK UNIT NUMBER
7. PERFORMING ORGANIZATION NAME(S) AND ADDRESS(ES) **Environmental Security Technology Certification Program U.S. Department Of Defense**	8. PERFORMING ORGANIZATION REPORT NUMBER
9. SPONSORING/MONITORING AGENCY NAME(S) AND ADDRESS(ES)	10. SPONSOR/MONITOR'S ACRONYM(S)
	11. SPONSOR/MONITOR'S REPORT NUMBER(S)

12. DISTRIBUTION/AVAILABILITY STATEMENT
Approved for public release, distribution unlimited

13. SUPPLEMENTARY NOTES
The original document contains color images.

14. ABSTRACT

15. SUBJECT TERMS

16. SECURITY CLASSIFICATION OF:			17. LIMITATION OF ABSTRACT	18. NUMBER OF PAGES	19a. NAME OF RESPONSIBLE PERSON
a. REPORT	b. ABSTRACT	c. THIS PAGE			
unclassified	**unclassified**	**unclassified**	**SAR**	**55**	

COST & PERFORMANCE REPORT
Project: MR-200603

TABLE OF CONTENTS

TABLE OF CONTENTS (continued)

Page

TABLE OF CONTENTS (continued)

Page

This page left blank intentionally.

LIST OF FIGURES

Page

LIST OF TABLES

Page

ACRONYMS AND ABBREVIATIONS

ANN	Artificial Neural Network
APG	Aberdeen Proving Ground
ATC	Aberdeen Test Center
ATV	all-terrain vehicle
BRAC	Base Realignment and Closure
CSV	comma separated values
DAQ	data acquisition
EM	electromagnetic
EMI	electromagnetic induction
EOD	explosive ordnance demolition
ESTCP	Environmental Security Technology Certification Program
EXP	mathematical expression
FUDS	formerly used defense sites
GDB	Geosoft database
GPS	Global Positioning System
GS	Geosoft Script
GX	Geosoft eXecutable
ha	hectare(s)
ID	identification
IDA	Institute for Defense Analyses
LBNL	Lawrence Berkeley National Laboratory
m^2	meter squared
m	meter
m/s	meters per second
MM	MetalMapper
MM/RMP	MetalMapper/RbstMultiPrince (inversion program)
μT	microtesla
NAVSEA	Naval Sea Systems Command
NF	no fins
NI	National Instruments
nT	nanotesla

ACRONYMS AND ABBREVIATIONS (continued)

OM	Oasis Montaj
P0	Polarizability at t = 0
$\mathbf{P}_d^{disc}$	Probability of Correct Classification
Pfp	Probability of False Positive
PC	personal computer
Pd	probability of detection
PO	program office
pts/day	points per day
QA/QC	quality assurance/quality control
RMS	root mean square
ROC	receiver operating characteristics
RTK	real-time kinematic
SERDP	Strategic Environmental Research and Development Program
SLO	San Luis Obispo
SNR	signal-to-noise ratio
TEM	transient electromagnetic
TOI	target of interest
USB	universal serial bus
UTM	Universal Transverse Mercator
UXO	unexploded ordnance
YPG	Yuma Proving Ground

ACKNOWLEDGEMENTS

The authors would like to thank the ESTCP Program Office for their support during this work. This work was also supported by the U.S. Army Corps of Engineers, Humphreys Engineering Center Support Activity under Contract No. W912HQ-06-C-0041.

This page left blank intentionally.

1.0 EXECUTIVE SUMMARY

The MetalMapper (MM) is an advanced transient electromagnetic (TEM) system for application towards the detection and characterization of unexploded ordnance (UXO). The antenna configuration includes three orthogonal transmitter loops and seven tri-axial receiver loops. The system can be deployed in mapping (or detection configuration) wherein it acquires data along profiles while the antenna platform is in motion. However, the most important benefit of the elaborate antenna configuration is that it permits us to characterize a buried metallic target from measurements at a single spatial point located (approximately) above the target. This system is being commercialized by Geometrics, Inc. (San Jose, CA).

In 2008, the MM was demonstrated at the Standardized UXO Technology Demonstration site located at Aberdeen Proving Ground (APG). In 2009 and 2010, the MM participated in live site demonstrations at the former Camp San Luis Obispo (SLO), and the former Camp Butner. The performance objectives of these demonstrations were to demonstrate the capabilities of the MM when operating both in its mapping mode (target detection) and in its static mode (cued ID target identification).

The system has a detection "footprint" of approximately 1 m^2, similar to that of the EM61. In detection mode surveying, the MM surveyed along parallel profiles with a nominal offset of 0.75 m. We acquired data at an average survey speed of less than 0.5 m/s in order to maximize data quality. At those speeds our average survey production was slightly more than 1 acre per day.[1] Analysis of detection scores and the MM data show that at these speeds we can detect targets down to a depth of 11 times the target diameter, as long as the detection threshold is chosen carefully. Simple threshold detection is clearly inadequate for instruments such as the MM, and improved methods are being developed in subsequent Strategic Environmental Research and Development Program (SERDP) projects, such as MR-1772. Static mode survey productivity is very much a function of terrain, navigation software, and deployment platform. Over the course of our three full demonstrations (APG, SLO, and Camp Butner), the productivity of the MM in the static mode doubled from approximately 200 points per day (pts/day) to over 400 pts/day, reflecting improvements both in our navigation software and in our deployment platform.

Our performance improved from one demonstration to the next. We attribute this improvement not to improvements in overall data quality but to improvements in our ability to identify and extract the important discrimination features from our static target data and in an improved understanding of the technology of decision theory and pattern recognition. At APG, for example, we achieved a discrimination score at our operating point of a Probability of Correct Classification ($\mathbf{P}_d^{disc}$) of approximately 90% at a Probability of False Positive (Pfp) of approximately 10% where the low probability of detection (Pd) primarily represented deep targets that were not detected by the MM.[2] In contrast, SLO discrimination scores were based

[1] Sample rate is typically 10 samples per second, and the MM survey speed can be easily doubled or tripled with a corresponding diminution of data quality and spatial sample density.

[2] To preserve the ground truth, the Aberdeen Test Center (ATC) scores provide only a depth range. Most of the targets not detected at APG lay in the depth range 8× to 12× the object diameter. At SLO, where we had the opportunity for a retrospective analysis, such targets were clearly seen in the data at levels below the chosen threshold. We believe the misses at APG were due to a similar cause.

only on detected targets. At SLO, the Geometrics' discrimination score at the operating point was Pd=98% with a Pfp≈5%. Using the same data, other "data processing demonstrators" generated similar results, thus showing that discrimination performance is not tied to a particular discrimination methodology. At Camp Butner, our discrimination scores were good, while those of some other demonstrators were nearly perfect. We conclude that the data quality gathered by the instrument is very high, and sufficient to support further work in processing of the targets for discrimination.

The estimated cost of deploying the MM based on the demonstrations we have conducted is high, two or three times what it would cost to deploy commercially available systems such as the EM61. These estimated costs are high because our demonstrations were conducted by-and-large with high-cost personnel, and we conducted field operations to maximize data quality rather than productivity. We project that the cost per crew day will drop substantially when the MM is routinely deployed and the labor costs drop. As it is now, the MM costs approximately $10,000 per hectare (ha) when used in the detection mode and $20/target when deployed for cued identification (ID). Detection mode productivity is about 0.5 ha/day; however, at normal survey speeds (~1 m/s), the detection mode productivity would be 1 ha/day. Cued ID mode survey productivity is 300 targets/day.

Higher costs and lower productivity in the detection mode can be justified only when we can demonstrate that through more advanced detection methods the MM can eliminate many superfluous targets such as small surface clutter. So far, however, we have not developed or applied advanced physics-based target detection principles and therefore we cannot justify any claims of superior target detection performance relative to simpler systems.

The demonstrated advantage of deploying the MM lies with its ability to discriminate targets and thus to produce a prioritized dig list. With regulatory acceptance, the use of a prioritized dig list would reduce the number of digs by 50% or more (depending on how conservative the dig policy was set). This would result in an overall cost savings of 30-40% in the cost of geophysical surveying plus digging. Therefore, the high cost for the deployment of the MM is justified on the basis that it can substantially reduce the cost of digging. However, routine deployment of the MM will require not only broad regulatory acceptance of this advanced electromagnetic (EM) technology but also that it or other advanced systems be specified for use in upcoming UXO remediation projects.

The MM is now a commercially available product from Geometrics. Geometrics is able to provide not only the basic hardware but also the software to support the data interpretation, as well as training and field support.

2.0 INTRODUCTION

2.1 BACKGROUND

There are millions of acres of land located at formerly used defense sites (FUDS) and military installations closed under the Base Realignment and Closure (BRAC) program. Much of this land has been contaminated with UXO. These lands must be decontaminated and restored before they can revert to civilian use. With present technology, the cost of the decontamination is estimated to be on the order of 10's of billions of dollars. The high cost for decontaminating these sites is driven by the need to visually identify all metal targets detected with current metal detecting technology. However, only a few percent of these targets are actually UXO. Because of the potential danger, these digs must be conducted by explosive ordnance demolition (EOD) technicians resulting in digging costs in excess of $100/target. At many sites, the target density can exceed 100 targets/acre. Development of technology that can reliably classify metal targets at a cost that is substantially less than the cost to dig can therefore substantially reduce the overall cost for decontaminating these sites by reducing the number of required digs [2].

The MM is an advanced electromagnetic induction system (EMI) configured for the detection and characterization of UXO. This technology represents a significant departure from existing commercially available EMI technology (e.g., the Geonics EM-61). Although the MM can be used in the survey or mapping mode for target detection, its most important application is for cued-ID target characterization. In the cued ID mode, data are acquired at one or more locations in close proximity to the target. Precision static measurements at these locations permit the calculation of the target characteristics. For isolated targets, a measurement at a single field point suffices. These target characteristics may be used to generate a prioritized dig list that can be used to identify targets that can with high confidence be left in the ground because they are not ordnance.

2.2 OBJECTIVE OF THE DEMONSTRATIONS

The primary objective of the demonstrations performed in this project was to gain acceptance of the MM system by the UXO community, including the regulators. To achieve this objective, we have shown by these blind demonstrations that the MM can indeed be used to reliably prioritize target lists for digging and significantly reduce the number of false positive (i.e., non-ordnance) items that need to be excavated.

2.3 REGULATORY DRIVERS

While there are no regulatory barriers to applying the technology embodied in advanced EMI systems such as the MM, the real problem is to convince regulators and other stakeholders of the reliability of the discrimination information that the MM can provide. The Environmental Security Technology Certification Program (ESTCP) program office (PO) is addressing this issue by conducting a series of blind live-site tests in which promising new technologies such as the MM are invited to participate. The demonstrations at Camp SLO and Camp Butner were two of these tests. To gain regulator acceptance, the PO has involved regulators in the site selection and other aspects of the test design.

This page left blank intentionally.

3.0 TECHNOLOGY

The MM was employed in full demonstrations at the Standardized UXO Technology Demonstration site at APG, at the former Camp SLO, and most recently at the former Camp Butner. A description is given in this section.

3.1 TECHNOLOGY DESCRIPTION

Geometrics is commercializing an advanced EMI system for UXO detection and characterization. Called the MM, the new system draws elements of its design from advanced systems developed by G&G Sciences, Inc. (supported by Naval Sea Systems Command [NAVSEA], SERDP, and ESTCP) and by the Lawrence Berkeley National Laboratory (LBNL) with support from SERDP and ESTCP.

3.1.1 MM Hardware

The MM system is unique and innovative in several respects:

- **Multiple Transmitter Loops:** The MM antenna platform includes 3 mutually orthogonal transmitter loops (see photo in Figure 1).
- **3-Axis Sensor Array:** The MM antenna platform includes an array of 7 3-axis receiver antennas, yielding 21 measurements of the secondary magnetic field.
- **Electronically Switched TEM Transmitter Loop Driver:** Under control of the data acquisition (DAQ) computer, the output of the transmitter can be directed to any single loop or automatically multiplexed between loops. Typically the loops are driven with a classical bipolar pulse-type TEM waveform (i.e., alternating pulse polarity with a 50% duty-cycle).

The photo of the MM shown in Figure 1 was taken during the demonstration that we conducted at the standardized UXO test site located at APG. During that demonstration, we towed the MM with a garden tractor in order to acquire dynamic data at a uniform survey speed. The system may be deployed on skids to minimize platform movement over undulating terrain. The antenna platform, including skids and optional wheels, weighs approximately 160 lb (72 kg) and can be moved by hand when necessary. At APG, cued ID (static) data were also acquired with the antenna platform deployed as a towed system. At SLO we mounted the MM in a skid connected to the front-end loader of a compact Kabota tractor. This deployment method improved our productivity for static data acquisition since it was easier to precisely locate the MM antenna over a static target site.

The DAQ is built around a commercially available product from National Instruments (NI). The DAQ, EM transmitter, and batteries for the entire system are packaged in an aluminum case that weighs approximately 43 lb when all four batteries are installed. For surveying, the aluminum case can be mounted on a pack frame, on a separate cart such as a hand truck, or on a vehicle such as an all-terrain vehicle (ATV) or lawn tractor (see Figure 1).

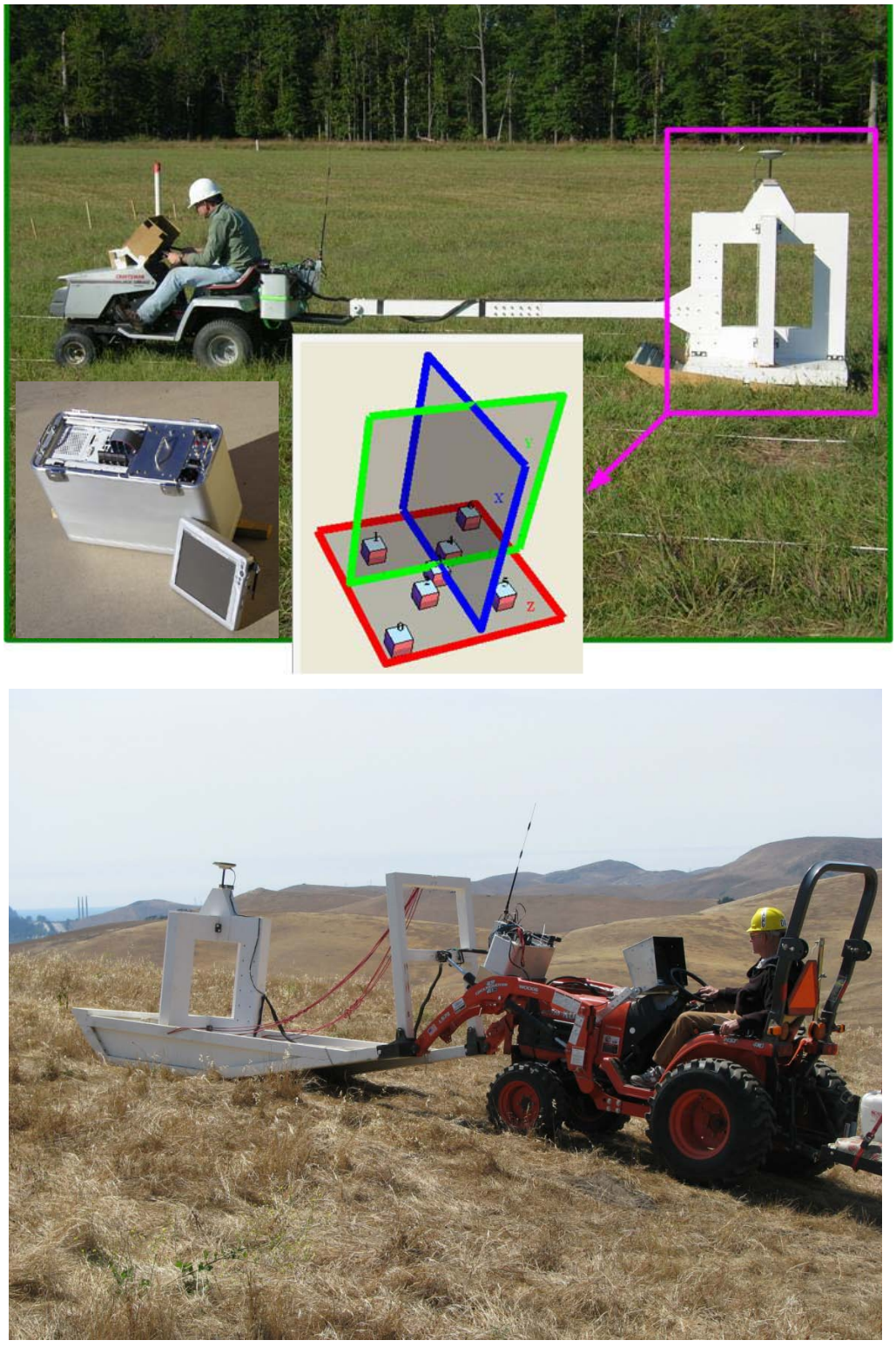

Figure 1. Photos showing the MM antenna array together with the electronics package and control console (inset above).
The top photo was taken at a demonstration conducted at APG. The bottom photo was taken at SLO.

The instrumentation package includes two external modules that provide real-time kinematic (RTK) global positioning system (GPS) and platform attitude (i.e., magnetic heading, pitch, and roll). The NI data acquisition system is a full-featured personal computer (PC) running Windows XP. It contains disk storage, serial and universal serial bus (USB) input/output ports, and more. It also contains a wireless link that allows the operator console to be remote from the DAQ.

3.2 ADVANTAGES AND LIMITATIONS OF THE TECHNOLOGY

The principal advantages of the MM system over existing commercially available EMI system are two-fold:

1. **Multitransmitter Target Illumination:** Because the MM has three orthogonal transmitter loops, it is able to illuminate or stimulate a target with primary fields from three independent directions from a single spatial field point. In contrast, single transmitter coil systems require the transmitter (and receivers) to be relocated to other field points so that the primary field will stimulate the target from a different direction. The concept is illustrated in Figure 2.
2. **Multiple Multi-Axis Receivers:** The MM employs multiple receivers. The MM receiver array consists of seven tri-axial receiver cubes measuring 10 cm on a side. With this array, the MM is able to sample the transient secondary vector field at seven unique spatial points. The positions of the receiver array are provided in Figure 4. The receivers are positioned so that they traverse profiles 13 cm apart along a survey line.

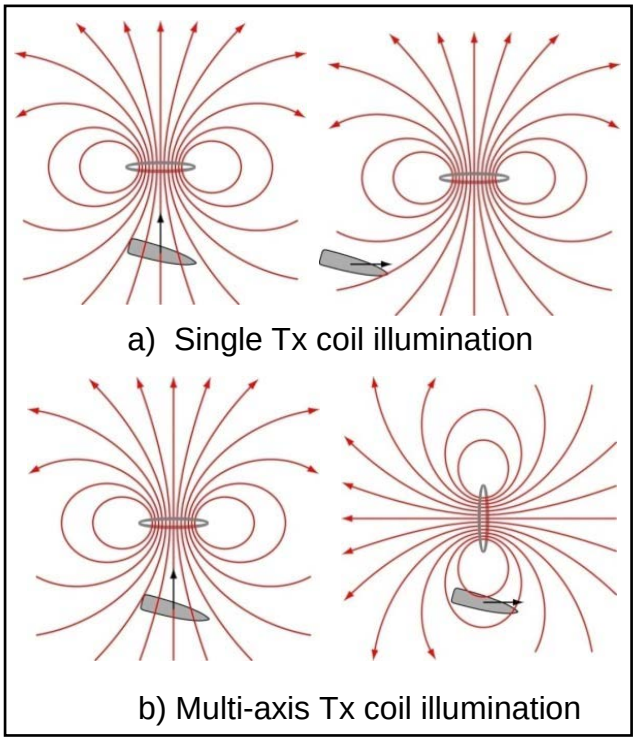

Figure 2. Figure contrasting the difference between single coil and multi-axis coil transmitter illumination[1].

This page left blank intentionally.

4.0 PERFORMANCE OBJECTIVES

We have conducted three full demonstrations (APG, SLO, and Camp Butner). We highlight here our results at SLO. Our objectives were as follows:

Table 1. Global SLO classification study performance objectives.

Performance Objective	Metric	Data Required	Success Criteria
Detection of all munitions of interest	Percent detected of seeded items	• Location of seeded items • Anomaly list	At least 98% of seeded items detected
Maximize correct classification of munitions	Number of targets of interest (TOI) retained.	• Prioritized anomaly lists • Scoring reports from the Institute for Defense Analyses (IDA)	Approach correctly classifies all TOI
Maximize correct classification of non-munitions	Number of false alarms eliminated	• Prioritized anomaly lists • Scoring reports from IDA	Reduction of false alarms by > 30% while retaining all TOI
Minimize number of anomalies that cannot be analyzed	Number of anomalies that must be classified as "unable to analyze"	• Demonstrator target parameters	Reliable target parameters can be estimated for > 90% of anomalies on each sensor's detection list
Dynamic Mode Survey Productivity	Area surveyed per day	• Field production log	>1.2 acre/day @ 0.75 m Lane spacing
Static-Mode Survey Productivity	Static pts/day	• Daily production logs	Pts >30/hr or Pts >200/day

4.1 OBJECTIVE: DETECTION OF ALL ITEMS OF INTEREST

Quality data should lead to a high probability of detecting the munitions of interest at the site. The metric for this objective is the percentage of seed items that are detected using the specified anomaly selection threshold. The objective will be considered to be met if at least 98% of the seeded items are detected.

4.2 OBJECTIVE: MAXIMIZE CORRECT CLASSIFICATION OF MUNITIONS

By collecting high-quality data and analyzing those data with advanced parameter estimation and classification algorithms, we expect to be able to classify the targets with high efficiency. The metric for this objective is the number of items on the master anomaly list that can be correctly classified as munitions by each classification approach. The objective will be considered to be met if all the items of interest are correctly labeled as munitions on the prioritized anomaly list.

4.3 OBJECTIVE: MAXIMIZE CORRECT CLASSIFICATION OF NON-MUNITIONS

By collecting high-quality data and analyzing those data with advanced parameter estimation and classification algorithms, we expect to be able to classify the targets with high efficiency. This reduces the number of false alarms. The metric for this objective is the number of items of interest on the master dig list that can be correctly classified as non-munitions by each

classification approach. The objective will be considered to be met if more than 30% of the non-munitions items can be correctly labeled as non-munitions while retaining all the TOI on the dig list.

4.4 OBJECTIVE: MINIMIZE NUMBER OF ANOMALIES THAT CANNOT BE ANALYZED

Anomalies for which reliable parameters cannot be estimated cannot be classified by the classifier. These anomalies must be placed in the dig category and reduce the effectiveness of the classification process. The number of anomalies for which reliable parameters cannot be estimated is the metric for this objective. The objective will be considered to be met if reliable parameters can be estimated for > 90% of the anomalies on each sensor anomaly list.

4.5 OBJECTIVE: HIGH DYNAMIC-MODE SURVEY PRODUCTIVITY

Operating in a vehicle-towed configuration, we surveyed the entire test area with the MM operating in its dynamic acquisition mode using a lane spacing of 0.75 m and a survey speed of 0.5 m/s (30 m/minute). Our objective was to complete the dynamic survey at a rate of 1 acre per day or more.

Since the MM antenna array contains seven tri-axial receiver cubes positioned so that each receiver cube tracks independent parallel profiles, the data from a single profile acquired with the MM can be split into seven individual profiles for the purpose of generating a very high resolution detection map (13 cm line spacing), even at a relatively wide 0.75 m line spacing of the vehicle track.

The metric for dynamic-mode survey productivity will be the average area covered per day.

4.6 OBJECTIVE: HIGH STATIC-MODE SURVEY PRODUCTIVITY

When operating in the cued ID or static survey mode, our objective is to maximize the number of sites visited per day consistent with maintaining data quality. Data quality is primarily a function of two variables in the field. First it is necessary to position the center of the antenna platform as nearly as possible to the desired target point. Second, data quality depends on the stacking time—longer stacking time means better data. Improving productivity therefore means decreasing both the time for target reacquisition and minimizing the stacking time.

For static-mode surveys, the metric will be targets/hr[3].

Our criterion for success for productivity in the static survey mode is 30 targets/hr. We achieved that level of production both at Yuma Proving Ground (YPG) and at APG. With the modifications we plan in our procedures and navigation software as well as in the way we mount the antenna platform to survey vehicle, we hope to improve on the productivity we achieved in our other demonstrations.

[3] We are adopting an hourly rate rather than a daily rate here because field days can vary significantly because of site access.

5.0 SITE DESCRIPTION

Over a one-year period, we have conducted demonstrations at the Standardized UXO Technology Demonstration Sites located at YPG, APG, Former Camp SLO in California, and most recently at Camp Butner in North Carolina. This Cost and Performance Report focuses mostly on the results of YPG, APG, and SLO, since the Camp Butner analysis was ongoing at the time this was written.

5.1 SITE SELECTION

The former Camp SLO, located near San Luis Obispo, CA, was carefully selected by the ESTCP PO as the demonstration site for classification study to be conducted in 2009. The MM was one of three advanced EM systems to participate in that study. The 12-acre study area is a former mortar and 2.36-inch bazooka rocket range. The site contains four munitions types of primary interest: 2.36-inch rockets, 60 mm mortars, 81 mm mortars, and 4.2-inch mortars. In contrast with the standardized UXO test areas at YPG and APG, the SLO demonstration area is situated on a hill and as such presents a significant challenge for survey in both detection or survey mode acquisition and in cued ID or static-mode acquisition.

5.2 SITE HISTORY

Camp SLO was established in 1928 as a facility for the California National Guard. It was used extensively during World War II as a training facility and again during the Korean conflict. The facility was inactive after the Korean conflict. At the present time, approximately half of the original land has been transferred to Cal Poly State University and Cuesta College, and the other half has been retained by the California National Guard.

5.3 SITE GEOLOGY

In contrast to the standardized test sites, topographic relief over the 12-acre SLO site is in excess of 200 ft with slopes sometimes exceeding 15%. Soil textures and thicknesses range widely. Thick sandy alluvium is found adjacent to washes and drainage channels. Thin to thick mountain terrace soils typically overlay crystalline metamorphic bedrock and are usually comprised of sandy to silty loam with a thin veneer of silty clay near the surface. Moisture levels vary seasonally. At the time of our demonstration (May-June 2009), the soils were very dry.

5.4 MUNITIONS CONTAMINATION

The SLO site is a live site. A preliminary dig of two small 50 ft $\times$ 50 ft grids in the 12-acre area of interest revealed 4 types of munitions: 2.36-inch rockets, 60 mm mortars, 81 mm mortars, and 4.2-inch mortars.

This page left blank intentionally.

6.0 TEST DESIGN

6.1 CONCEPTUAL EXPERIMENTAL DESIGN

Each of the field demonstrations was conducted in three phases:

1. Dynamic-mode survey for target detection
2. Static-mode survey for cued-ID discrimination
3. Post-acquisition analysis.

The Gantt chart in Figure 3 provides a timeline for the demonstration and also serves as an outline for the various activities involved.

C) Activities – MetalMapper SLO Demonstration (May-Jun 2009)

ID	Task Name	Start	Finish	Duration
1	Mobilization	5/23/2009	5/24/2009	2d
2	Setup	5/25/2009	5/25/2009	.5d
3	Det Survey	5/25/2009	6/1/2009	7.5d
4	Static – Tst Pit & Tst Strip	6/3/2009	6/3/2009	.5d
5	Break	6/4/2009	6/7/2009	4d
6	Static Tests	6/8/2009	6/8/2009	.5d
7	Cued ID Survey	6/8/2009	6/15/2009	7d
8	Repeat Dyn Survey	6/15/2009	6/16/2009	.5d
9	Repeat Static Survey	6/16/2009	6/16/2009	1d
10	Take Down/Demob	6/17/2009	6/18/2009	2d
11	Field Processing QA/QC	5/25/2009	6/17/2009	24d

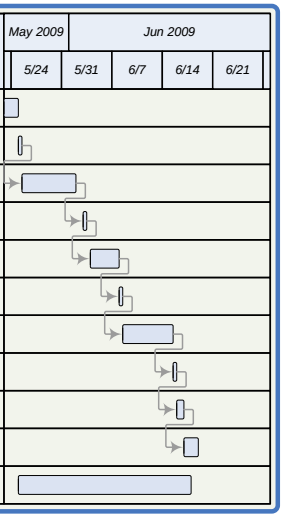

Figure 3. Gantt charts providing timelines and activity breakdowns for MM demonstration covered in this report.

6.1.1 Target Detection (Mapping Survey)

In the first phase of each field demonstration, the MM was operated in its dynamic (mapping) mode in order to generate a detection map. In its dynamic mode, only the horizontal (Z) transmitter loop is energized. Data are acquired along a series of parallel profiles with 0.75 m (nominal) line separation. These data are compiled into a detection map wherein the mapped parameter indicates a peak centered directly over any metallic target within range. Peaks were chosen (i.e., "detected") either manually using the computer mouse or automatically using an automatic peak detector that operates on a data grid. In all cases where an automatic peak detector is employed, it was necessary to edit the resulting peaks in order to remove or "merge" multiple target picks on the same anomaly. The resulting edited target list was used during the next (cued ID) phase of the demonstration.

6.1.2 Cued ID (Static Survey)

The target list generated from the mapping survey is "cued" (sequenced) so that each target can be efficiently reacquired. Reacquisition requires that the antenna platform be nominally centered over the anomaly of interest. Once a target is reacquired, the MM is activated to acquire a single static data set. For static data acquisition, each of the three transmitter loops is energized while data transients are measured from the seven triaxial cube receivers (21 transients). Because the antenna platform is motionless, each receiver transient can be repetitively stacked over many cycles of the transmitter, thus significantly reducing incoherent random noise. A complete data set that includes the results from energizing each of the three transmitter loops takes 25-50 seconds, depending on the stacking parameter.

6.1.3 Post-Acquisition Analysis

Preliminary data processing for the purpose of generating detection maps and for quality assurance/quality control (QA/QC) purposes is carried out throughout the course of the field demonstration. However, most of the data processing required to assemble a target list for scoring occurs after the field activities have been completed (post-acquisition). Post-acquisition processing includes the following six steps:

1. **Target Association:** Static data points are associated with a particular target site on the basis of proximity.
2. **Feature Selection:** Statistical analyses including scatter plots, principal component analysis, and trial and error are performed to help select a set of features (feature vector) associated with the targets that we think best identifies the TOI from clutter.
3. **Library Matching:** Generate a library of "type" polarization curves representing the munitions types known to exist in the area of interest. Match the polarization curves extracted from each of the unknown targets with those in the type library. Select the target type with the best matching score.
4. **Neural Network Training:** Train a neural network using feature vectors corresponding to targets for which ground truth is available.
5. **Neural Network:** Apply feature vectors from each target in the test set (i.e., all unclassified targets) to the neural network trained in Step 4.
6. **Target List Assembly:** Finally, the results from both library matching and neural network analysis are merged to form a single classification score.

6.2 SITE PREPARATION

The standardized UXO sites have been seeded with inert munitions according to procedures reported in a handbook assembled as part of the Standardized UXO Demonstration Program [3]. Unlike the standardized test sites at APG and YPG, Camp SLO is a live site. Preliminary investigations included a magnetometer transect survey and an EMI survey over a larger area to assist in selecting a smaller site suitable for the discrimination study. In addition, two small 50 ft $\times$ 50 ft grids were dug in order to identify the munition types that would likely be encountered

during the SLO study. Finally, additional munitions of the type expected at SLO were seeded in order to increase the ratio of TOI to clutter items.

6.3 SYSTEM SPECIFICATION

6.3.1 Antenna Platform

The MM's three transmitting loops are positioned as follows:

- Z transmitter (coil axis vertical): 1 m × 1 m, center is ~21 cm above ground level. The center of the Z loop is taken to be the local origin of coordinates for the cart.
- Y transmitter (coil axis horizontal in direction of travel): 1 m × 1 m, centered 0.56 m above the origin.
- X transmitter (coil axis horizontal, clockwise from Y): 0.98 m × 0.98 m, centered 0.56 m above the origin.

The MM's seven receivers are positioned as shown in Figure 4. Note that the seven receivers traverse profiles that are 13 cm apart in the cross-track (x) dimension.

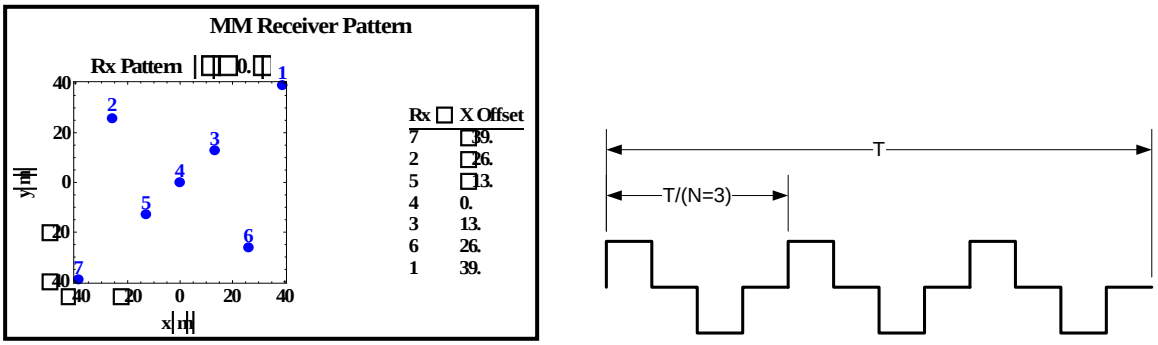

Figure 4. MM receiver locations.
All seven receivers are in the plane of the horizontal transmitter (Z) loop (above left). Above right shows an MM acquisition block illustrating a bipolar transmitter waveform with 50% duty cycle and a repeat factor (N) of 3. Block periods are operator selectable from 33.333 ms to 0.9 s in multiplicative steps of 3.

6.3.2 Data Acquisition: Dynamic Data

To collect dynamic data, the MM is operated in continuous mode, and all data from a single survey line are stored in a single file.

6.3.3 Post-Acquisition Data Processing: Dynamic Data

Data are stored as binary formatted files. The processing software includes the capability to export the data to a Geosoft Oasis Montaj (OM) database and/or to text files. For dynamic surveys, OM is used for display, QC, map compilation, etc.

As we indicated in Section 4 of this report, we follow a two-step approach to target characterization. The first step is target detection and for that we conduct a dynamic survey. Using a custom Geosoft eXecutable (GX), the data from the dynamic survey are imported into a Geosoft database (GDB). Other custom GXs have been developed to process the transient data to a point where they can be further processed and displayed using standard capabilities within the Geosoft Montaj software package. The end products of the post-acquisition processing of the dynamic data are target detection maps and profiles and a list of detected targets along with their respective X-Y coordinates. In Figure 5, we show the detection map that we generated from dynamic data acquired over the Blind Grid at APG.

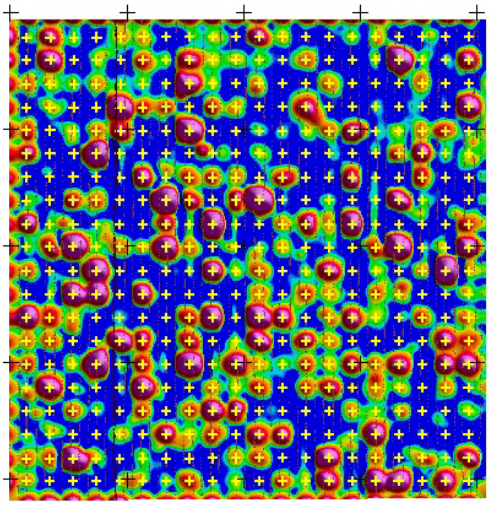

Figure 5. Target detection map – Blind Grid.
MM demonstration at APG (September 2008).
The "+" symbol denotes the center of a 2 m × 2 m cell.

6.3.4 Post-Acquisition Processing: Static Data

Static data points are acquired with the MM platform located over each of the targets identified using the dynamic data as described above. These data files are processed with our physics-based modeling program MM/RbstMultiPrince (MM/RMP) (inversion program) to extract target-specific parameters.

6.4 CALIBRATION ACTIVITIES

Calibration checks of the MM system were performed at least two times per day as part of our routine QA/QC procedure. At SLO, the dynamic calibration was performed over the Calibration Strip. A check on the static measurement was performed using a steel sphere located in the calibration pit. The calibration procedure is enumerated below:

1. Acquire a static background data set over a designated "background" point (typically a designated point at the beginning/end of the Calibration Strip.
2. Acquire dynamic data over the calibration strip in reciprocal directions using our standard dynamic survey acquisition parameters

3. Acquire a static data set with the antenna platform centered over a steel sphere located in the Test Pit.

The calibration procedure provides all the data required to perform a variety of QA/QC checks that document that the instrument is functioning correctly. Moreover, the resulting data was also used to establish the long-term stability of the instrument response.

6.5 DATA COLLECTION

We surveyed the entire 11.8-acre study area at SLO with the MM operating in detection mode. Using maps from these data, we selected 2178 targets for cued ID measurements. We also repeated cued ID measurements over 314 of these targets based on inversion results that indicated that the horizontal offset of these targets was greater than 0.4 m. We submitted a detection target list containing a total of 1638 target picks. We were able to associate at least one MM static file with 1617 picks.

6.6 VALIDATION

Camp SLO is a live site. Detected items were dug by Parsons, Inc. under contract with ESTCP. Parsons, Inc. utilized standard procedures for digging UXO live sites. In addition, the position, depth, approximate attitude, and a photograph of the resulting target found were recorded. The results of the first five 30 m $\times$ 30 m survey blocks were provided to all data processing demonstrators for use as training data. The remainder of the dig results were held in confidence by the program officer and IDA and used for the purpose of scoring discrimination target lists prepared by the demonstrators according to protocols described in a scoring memorandum prepared by the IDA and distributed to the demonstrators [4].

This page left blank intentionally.

7.0 DATA ANALYSIS AND PRODUCTS

7.1 PREPROCESSING

7.1.1 Dynamic Survey Data

The dynamic survey data consists of parallel profiles acquired with 0.75 m offsets. Each profile is recorded to a separate binary data file. From these data, we compiled detection parameter maps of the surveyed area or sub-area. The detection map is based on the magnitude of the secondary fields measured at each of the seven tri-axial receiver sensors. The following processing steps, accomplished using Geosoft OM, are required:

1. MM data are recorded as binary files. These data are imported directly into an OM database where simple editing is performed (editing line numbers, deselecting duplicate lines, trimming and deleting bad data or stops, etc). All other steps are accomplished from within OM using its standard editing and processing capabilities supplemented where necessary with custom GXs, Geosoft Scripts (GSs), and Geosoft mathematical expression (EXP) files.
2. Convert latitude and longitude to Universal Transverse Mercator (UTM) coordinates, and make a true heading channel from the UTM coordinates. Edit and filter pitch and roll channels. Compute corrected UTM coordinates according to heading, pitch, and roll.
3. Compute detector gate values for each of the 21 receiver channels. The detector gate value is the value of the recorded transient integrated optionally with an exponential weighting function over a selected time interval.
4. Compute transmitted current by gating (windowing) the transmitted current transient.
5. Select and remove background (leveling).
6. Generate vector magnitude channels for each of seven tri-axial receiver cubes
7. Split each profile into seven separate profiles, corrected for heading and offset distance from the platform measure point (generates seven parallel profiles with 13 cm offsets).
8. Grid the resulting amplitude data, applying grid smoothing filters if necessary.

Steps 1-5 in the above numeration constitute preprocessing steps that result in data that can be exported for delivery to the PO and analysis demonstrators.

7.1.2 Static Data

As we stated previously, raw static data files are input directly into MM/RMP together with an appropriate background file and a file containing root mean square (RMS) noise estimates for each channel and time gate. What we have heretofore termed “preprocessing” (e.g., location correction, background removal, etc.) is performed within MM/RMP during the parameter extraction process. Preprocessed data were required only during the SLO demonstration.

During that demonstration, there were several organizations that needed these data to independently prepare discrimination target lists. We modified MM/RMP so that it can output preprocessed static data files in comma separated values (CSV) format as specified by the PO. The data files were delivered to the PO and subsequently distributed to other demonstrators.

7.2 TARGET SELECTION FOR DETECTION

Guidance from the ESTCP demonstration plan for the SLO Classification Study required that all targets be picked on the basis of anomaly threshold. The applicable detection threshold was to be determined by studying the predicted and measured response for the four principal TOIs at SLO, which are the 60 mm/81 mm/4.2-inch mortars plus the 2.36-inch (bazooka) rocket. Our detection threshold was based on the predicted response of the smallest of the four TOIs when placed in its least favorable orientation (horizontal) when buried at a depth of interest of 45 cm below ground. We generally followed the methods and rationale developed by Nelson, et. al. [5] in determining the threshold to apply for target detection at SLO. First, we computed average polarizability transients for the four TOIs. We computed these averages using static data sets that we measured with the MM over the four TOIs. We were able to use data from YPG and APG for the 60 mm and 81 mm mortars. We used approximately 15 data sets for each target type representing a range of depths and orientations with respect to the antenna platform. The results are shown in Figure 6. The smallest detection threshold was about 3 nanoteslas (nT)/s for the horizontal 2.36-inch rocket at a depth of 0.66 m below the platform (0.45 cm below ground level).

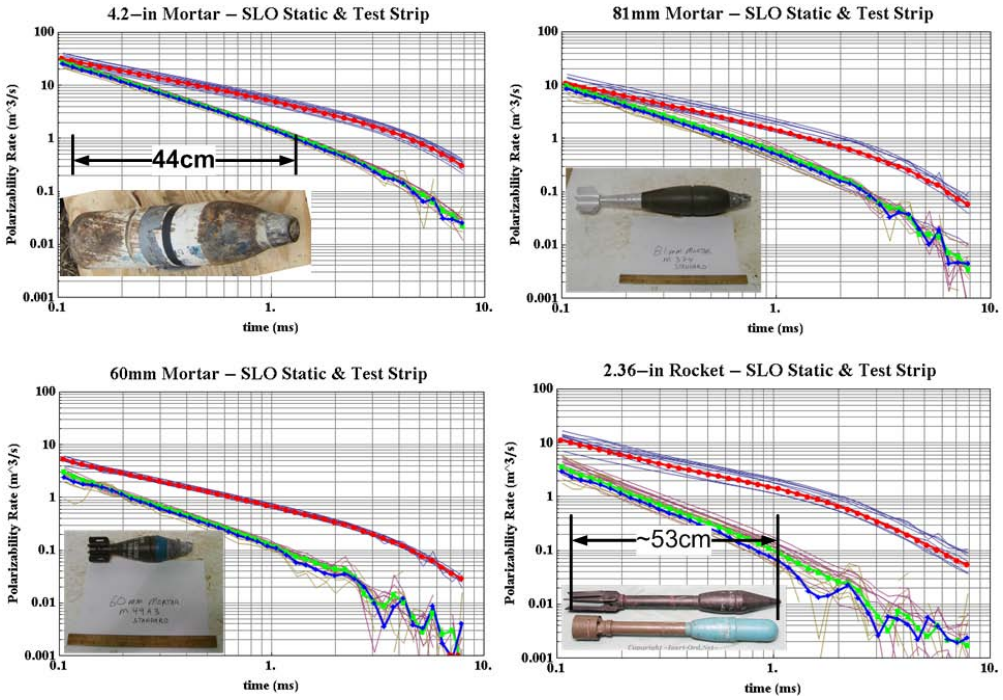

Figure 6. The average principal polarizability curves (red, green, blue) for the four principal TOIs at Camp SLO.

These curves were derived from approximately 15 independent static MM measurements acquired in the free air (SLO Test Pit), and in the ground (SLO Test Strip). The average curves were used in estimating the target detection threshold to be used at SLO.

7.3 PARAMETER ESTIMATES

The conceptual processing flow is illustrated in Figure 7. The figure shows the 63 transients comprising a data set on the left. The panel on the right shows the three principal polarizability rate transients. We call the computer program that accomplishes this transformation MM/RMP. The basis of MM/RMP is the ubiquitous point dipole model approximation for approximating the EMI response of a small conducting and magnetically permeable object. By-products of this modeling process are estimates of the target position and attitude angles. The dipole model approximation is widely used within the UXO community for interpreting UXO [6]-[10]. A particularly thorough and systematic treatment of the theory can be found in Chapter 2 of Leonard Pasion's Ph.D. thesis [11]. The algorithm used in MM/RMP was developed by J. Torquil Smith at LBNL [12]. The basic theory for the dipole approximation of EMI response for small objects is summarized in Figure 8. We outline the essential elements of the theory below:

1. We can approximate the behavior of the target as a point dipole characterized with a time- or frequency-dependent polarizability tensor (P).

2. The primary magnetic field (Hp) "illuminates" the target object, which is assumed to be very highly conducting and (possibly) permeable. In Figure 8, the primary field is generated by transmitter loop (red) carrying a time varying current.

3. As suggested in Figure 8, the polarizability tensor P is a second rank symmetric tensor having six independent elements. In such cases, there exists a coordinate system called the "principal axes" coordinate system in which the polarizability tensor is diagonal with only three elements. The "principal axes" coordinate system and the observation coordinate system are related by means of an orthogonal transformation (T). The orthogonal transformation can be expressed in terms of three elementary rotation angles (φ,θ,ψ) sometimes called the "Euler Angles." At any particular time or frequency, the response at the receiver is a function of nine parameters: 1) the three coordinates of the target position, 2) the three Euler Angles, and 3) the three diagonal elements of the polarizability tensor evaluated at a particular time or frequency.

4. Given sufficient independent measurements of the secondary field B, one can estimate the nine unknown parameters enumerated in 6 parameters using well-known principles of nonlinear and/or linear inversion.

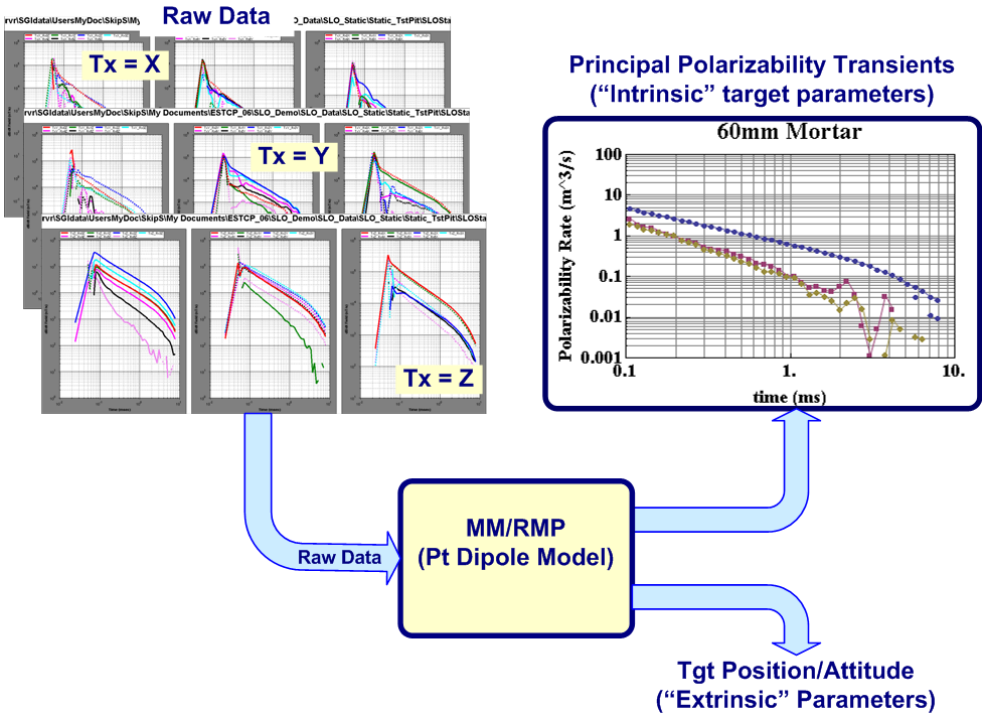

Figure 7. Parameter extraction using MM/RMP.
The input data are transients (63) acquired during a single static-mode measurement with the MM. The outputs are the principal polarizability rate transients, target position, and target attitude.

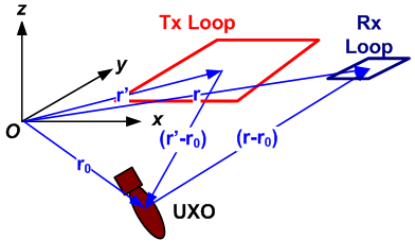

$$\dot{\tilde{\mathbf{B}}}\left(\vec{\mathbf{r}}-\vec{\mathbf{r}}_0,\vec{\mathbf{r}}_0-\vec{\mathbf{r}}';t\right)=\mu_0\tilde{\mathbf{G}}\left(\vec{\mathbf{r}}-\vec{\mathbf{r}}_0\right)\cdot\left\{\dot{\tilde{\mathbf{P}}}(t)\cdot\vec{\mathbf{H}}^{p}\left(\vec{\mathbf{r}}_0-\vec{\mathbf{r}}'\right)\right\}$$

$\vec{\mathbf{r}}$ = Rx position; $\vec{\mathbf{r}}'$ = Tx position; $\vec{\mathbf{r}}_0$ = target position

$\tilde{\mathbf{G}}\left(\vec{\mathbf{r}}-\vec{\mathbf{r}}_0\right)=$ Dipole Green's function

$\dot{\tilde{\mathbf{P}}}(t)$ = Polarizability rate tensor (symmetric w/ 6 unknowns)

$$\dot{\tilde{\mathbf{P}}}=\begin{bmatrix}\dot{p}_{11} & \dot{p}_{21} & \dot{p}_{31}\\ \dot{p}_{21} & \dot{p}_{22} & \dot{p}_{32}\\ \dot{p}_{31} & \dot{p}_{32} & \dot{p}_{33}\end{bmatrix}=\tilde{\mathbf{T}}^{\mathrm{T}}(\phi,\vartheta,\psi)\cdot\begin{bmatrix}\dot{p}_1'(t) & 0 & 0\\ 0 & \dot{p}_2'(t) & 0\\ 0 & 0 & \dot{p}_3'(t)\end{bmatrix}\cdot\tilde{\mathbf{T}}(\phi,\vartheta,\psi)$$

$\vec{\mathbf{H}}^{p}\left(\vec{\mathbf{r}}_0-\vec{\mathbf{r}}'\right)$ = Primary magnetic field intensity (function of $\vec{\mathbf{r}}_0$).

$\tilde{\mathbf{T}}(\phi,\vartheta,\psi)=$ Orthogonal transformation (3 unknowns)

$\dot{p}_1'(t),\dot{p}_2'(t),\dot{p}_3'(t)$ = Principal polarizability transients

Figure 8. Summary of the theory for approximating the response of a small conducting and permeable object with a point dipole.

7.3.1 Meta-Parameters

Scalar Meta-Parameters—Many have found success with target discrimination using scalar parameters derived from much simpler instruments. Moments of the principal polarizability transients are easy to compute numerically and very robust with respect to noise. We have benefitted from the insight on the relationship of moments to meaningful target features provided in a paper by Smith and Jones [13]. Mathematically, the nth moment of the polarizability is defined as

$$P_n = \int_0^\infty t^n P(t)\,dt \text{ ; where } P(t) \text{ is a polarizability rate transient.}$$

We calculate the 0^{th} and 1^{th} moments for each of the three principal polarizability transients thereby producing six scalar "meta-parameters" (P_{0x}, P_{0y}, $P_{0z,}$ P_{1x}, P_{1y}, P_{1z}) where the subscripts (*x, y, and z*) denote the principal axes coordinates.

For each of these scalar parameter sets (P_0, P_1), we calculate two additional scalar values, two of which relate to target shape:

1. **Target Aspect:** $P_{iR} = \frac{P_{ix}}{P_{iT}}; i = 0,1$ —This is a measure of the aspect or elongation of the target. Values of P_{iR}>1 suggest rod-like targets while P_{iR}<1 suggest flat targets.
2. **Target Eccentricity:** $P_{iE} = \frac{(P_{iy} - P_{iz})}{P_{ix}}; i = 0,1$ —This is a measure of the eccentricity of the target. A target with good symmetry with respect to the principal *x* axis will have P_{0E}<<1.

7.4 CLASSIFIER AND TRAINING

Discrimination starts with the estimation of target-related parameters from our data. When viewed in the principal coordinate system, the polarizability of a UXO will manifest itself by exhibiting a single large (major) polarizability transient over two smaller (minor) transients. Clutter-like objects do not exhibit such symmetry properties.

With good data, an interpreter can easily discriminate between items that are most likely TOIs and items that are most likely clutter. The visual (and numerical) clues are:

- **Object Size—**Size as suggested by the three scalar values (P_{0x}, P_{0y}, P_{0z}) can be used to narrow the possibilities to one of three size classes.
- **Symmetry (Eccentricity)—**In most cases, the principal polarizability curves should indicate a rod-like body having a large major polarizability curve and two smaller minor polarizability curves of roughly the same size and shape. This is the case for all examples we have shown thus far. Note that the symmetry or eccentricity property is a function of time.

- **Aspect Ratio—**This is the ratio of the major curve to the geometric mean of the minor curves and is a function of time.
- **Major Polarizability Shape—**The shape of the largest principal polarizability curve is often very distinctive.

7.4.1 Artificial Neural Net (ANN) Classifier

We used an ANN to generate a binary decision regarding whether a particular target is a TOI or not. We needed to choose a set of feature parameters from the data to feed to the neural network. For this purpose, we used the commercially available software package, Statistica version 6.0/9.0. We analyzed scalar polarizability parameters extracted from static MM data sets collected over 2177 targets.

Our objective was to combine a basic statistical analysis of the data with expert knowledge about the data and the ANN choice of parameters to select a subset of parameters to use for the ANN analysis. Input parameters should be selected to provide the best separation between clutter and TOI signatures. In order to keep the number of connection weights in the ANN small, we want to identify the smallest set of input parameters that can provide effective classification.

We visually classified 2177 targets as UXO or clutter. Next we looked at the correlation of parameters. Ideally we want parameters that are not correlated with each other as input parameters since this means they include redundant information. Next, we looked at the sensitivity of the classification to the input parameters. We ran several trials and measured in how many trials particular features were considered important. Our final feature vector includes nine robust parameters that capture (in scalar form) the properties of target size (polarizability at t=0 [P0] – 3 axes), target aspect (P0_R), target symmetry (P0_E), and target polarizability time persistence (P1/P0 – 3 axes):

(P0x, P0y, P0z, P0R, P0E, P1E, P1x/P0x, P1y/P0y, P1z/P0z)

After the results of the training dig were distributed to those involved in the classification processing, we had just sufficient data so that we were able to train a network totally on data for which the ground truth was known.

7.4.2 Target Types for Library Matching

We supplemented the ANN processing with a library matching algorithm in order to identify some items that were missed by the neural network. Initial reconnaissance dig information, later buttressed by results from the training dig, identified four primary TOI types. We developed our initial “type” polarizability curve library from the static measurements we acquired with the MM in the test pit and the test strip. Using the specimen targets provided at SLO we measured the free-air response of each target placed at four different attitudes and two different depths. In addition, we acquired static measurements over a specimen of each target type buried in the calibration strip several times during the course of our demonstration.

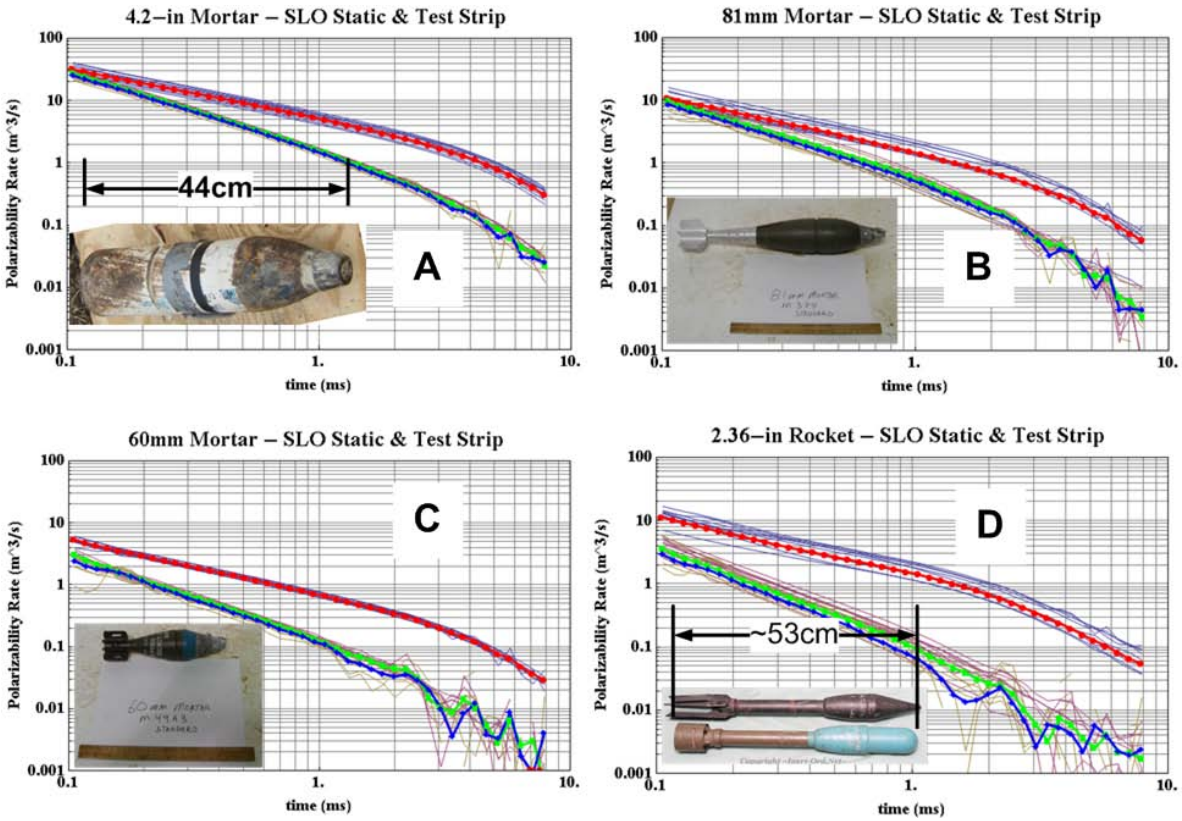

Figure 9. Principal polarizability curves for the four munitions of primary interest at SLO. Each curve set is derived from an ensemble of 14 static measurements over targets at different depths and orientations. The heavy curves (red/green/blue) are the geometric mean curves computed by taking the geometric mean of their respective ensemble.

7.4.3 Classification Results—Training and Test

As we indicated above, we ended up training two networks:

1. **ANN Network 1:** This ANN was trained with test pit and test strip data (58 data points), data from the test dig (208 points), and 12 data points that were visually classified as 60 mm no fins (NF). Although we had MM static points associated with only 154 of the targets in the training dig, many of those targets had two or more MM data points associated with the target. By using these (54) repeated data points, we "augmented" our training set so that it had 278 targets.
2. **ANN Network 2:** This ANN was trained with a total of 563 targets comprised of the 58 points from the test pit and test strip, the 208 points (as above) from the training dig, and 296 points that were visually classified.

Figure 10 shows the receiver operating characteristics (ROC) curves that result from applying the two ANNs to their respective training data. Note that in both cases, the ANN leaves a few "hard" false negatives that would require us to dig a high percentage of all the targets before digging the last TOI. However, after applying the library matching, the hard false negatives are moved closer to the knee (operating point) of the curve, thereby dramatically reducing the

number of targets we need to dig before we dig the last TOI (100% detection point). However, the major benefit of using library matching is that it reduces the number of false negatives.

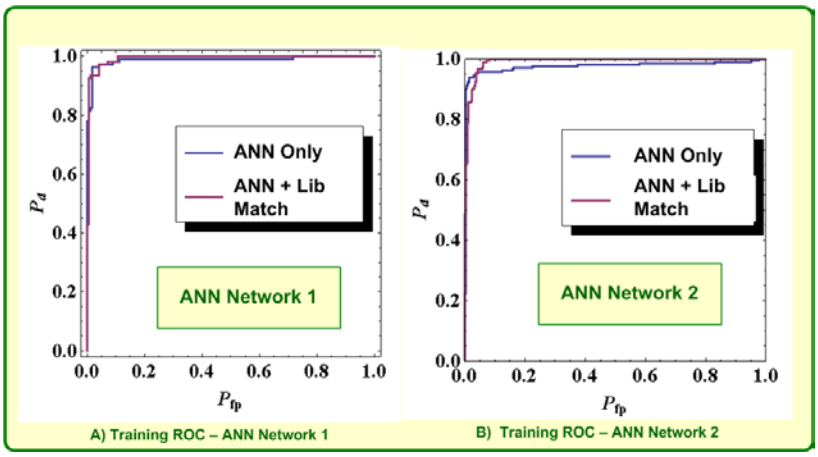

Figure 10. ROC curves showing the results of applying ANN and the ANN + library curve matching to their respective training sets after training.
The curve library contains five types (60 mm, 60 mm NF, 2.36-inch, 81 mm, 4.2-inch).

7.5 DATA PRODUCTS

The principal data product arising from the processing is a prioritized dig list that can be scored against ground-truth. We have tried to emphasize throughout this section that our procedures and ability to construct a prioritized dig list have evolved during the course of the three demonstrations we have conducted and have reported on here. Indeed, the SLO demonstration has led us to develop and document each step in the classification process.

While the prioritized dig list is the primary product of the demonstrations, there are also many other data products required in order to adequately document and measure the performance of the MM against the various performance objectives that we have enumerated in Section 4.

8.0 PERFORMANCE ASSESSMENT

In this section we will assess the performance of the MM system against the performance objectives contained in Table 1.

8.1 TARGET DETECTION

At SLO, there were 187 seeded targets. The MM failed to detect four of those seed targets. The four targets we missed were all 60 mm mortars. Therefore, we achieved the stated performance goal of Pd >= 98%.

It is instructive to look at the reasons we failed to detect these four targets (SLO targets 59, 478, 410, and 16). All four were 60 mm mortar bodies. Target 410 is typical of the other three. The issue is summarized graphically in Figure 11. The anomaly is obvious in both the map and the profiles. But it fails to rise above the experimentally verified detection threshold. The "expert" interpreter would have recognized this anomaly as likely arising from a deep target because of its broad extent and coherence, notwithstanding its low amplitude. A look at the recovered target object (Figure 12) explains why this target had a lower detection signal amplitude than we expected for a 60 mm object. The seeded target was a 60 mm mortar (body only) target. We defined the detection threshold based on the signal amplitudes for a 60 mm M49A4, the type of 60 mm mortar seeded at APG and YPG, buried in the test lanes at SLO, and provided at SLO for free-air tests. The mortar body target has an electromagnetic size that is approximately half the size of the complete mortar including fins and a fuse. Obviously, the detection threshold was set too high. However, had we set the threshold to 1 uV/Am2 we would have easily doubled or perhaps tripled the number of targets detected.

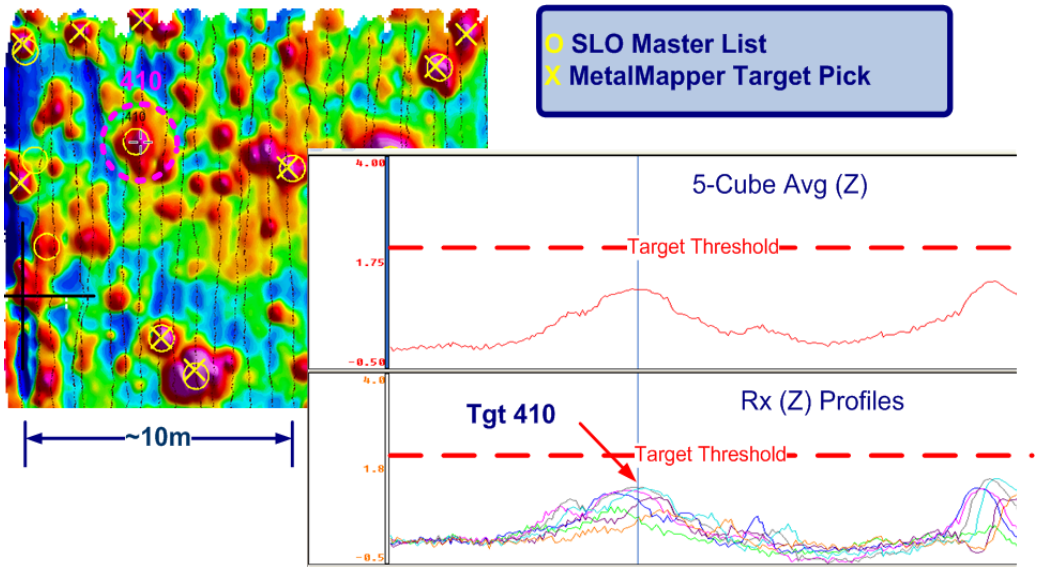

Figure 11. Figure showing one target that went undetected in the MM dynamic survey.
Target 410 is readily discernible on both the map and the profiles. Although it has a broad areal extent indicating a deep target, its amplitude fails to rise above the detection threshold.

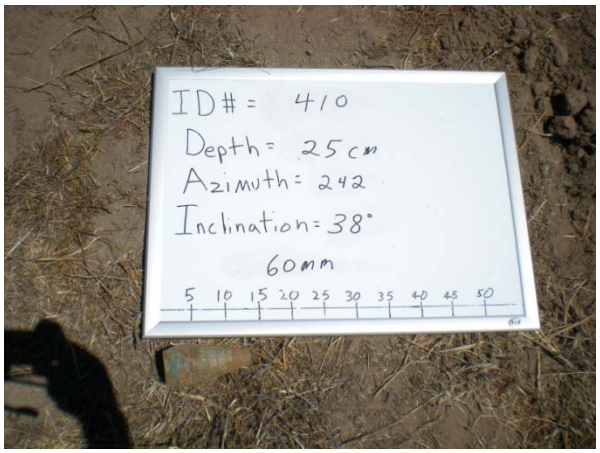

Figure 12. Photograph of the recovered 60 mm "body" associated with SLO target number 410.

8.2 ANALYSIS AND CLASSIFICATION PERFORMANCE

The SLO project permitted us to develop a methodology that achieves the performance objectives set out in the ESTCP demonstration plan. We base the following discussion on the scoring results that we received from IDA in early November 2009. In Figure 13, we have reproduced and annotated the IDA ROC curves. These ROC curves summarize the scoring results representing a partial dig (106[4] items from a list of 1408) of the MM target list.

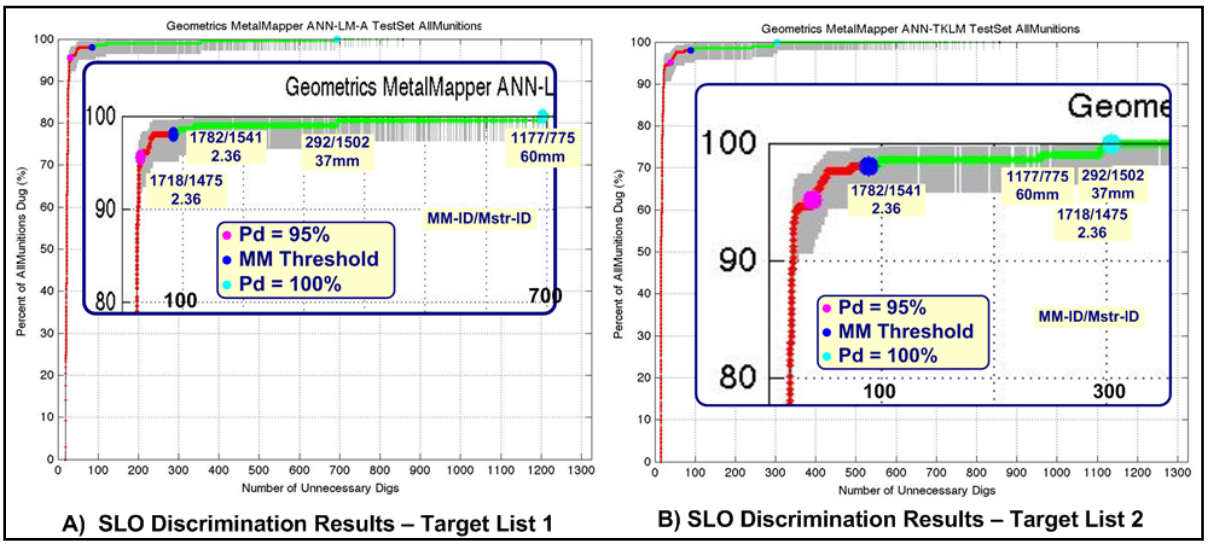

Figure 13. IDA ROC curves for the two discrimination stage target lists submitted in connection with the SLO classification study.

The differences in the lists are the result of using different data sets for training the ANN and different versions of the ANN software. In the insets, we have identified the four false negative targets that occur beyond the MM threshold. Note that the same four targets are involved in both target lists (albeit in different order).

[4] The test data used by IDA consists of 1064 targets of which 206 were designated TOI and the balance (858) as clutter or non-ordnance items.

8.2.1 Maximize Correct Classifications—Munitions (see Section 4.2)

The ROC curves (Figure 13) show that at our operating threshold we had four false negatives, two of which were very "hard" in the sense that our classifier indicated that it was highly probable that these objects were clutter.

We have examined the dig results from the four targets associated with the hard negatives. In the expanded ROC curves (inset Figure 13, A and B) the four targets are identified according to their MM ID and Master List IDs, respectively, with the "/" character as a separator.

8.2.1.1 MM-ID 292/Master ID 1502 (37mm)

The 37 mm target is the only target that is an obvious "miss" that could have (should have) been avoided by a comprehensive visual examination of the polarizability curves. In both target lists, the 37 mm target (the only one in the test data set) was very strongly identified as clutter (non-munition). The problem is that our classifier was not trained to identify a target of the size and shape of the 37 mm. In a retrospective study, we added the polarizability curves for a 37 mm from our library of munitions types for APG (see Figure 14). Our library matching algorithm identified the 37 mm with very high probability. Therefore, we conclude that we will be able to detect and classify 37 mm targets using library matching provided we add a 37 mm type to our matching library (a sixth type) and that we include specimens of the nine-component feature vector extracted from static measurements of 37 mm projectiles.

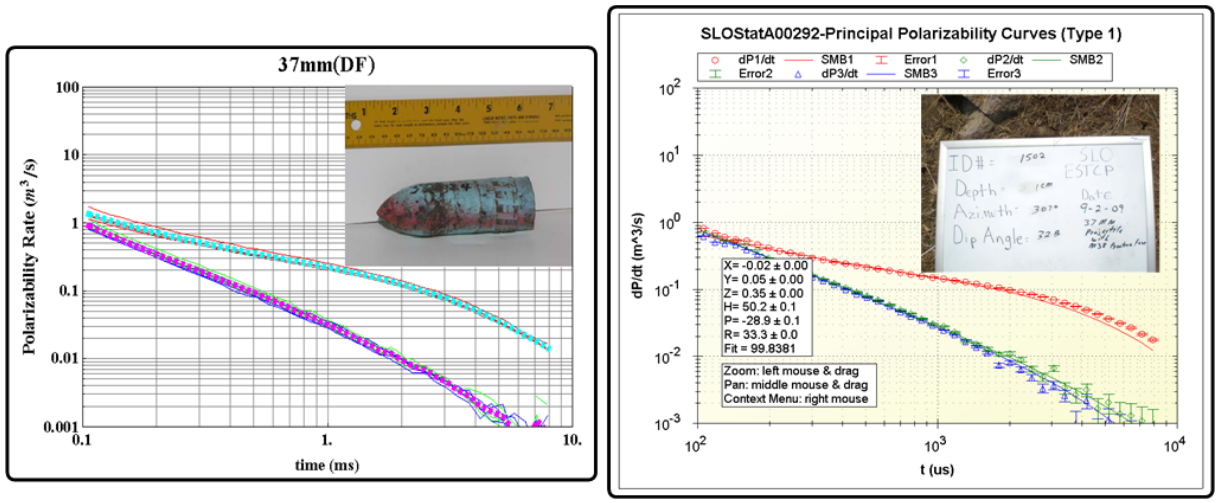

A) 37mm "Type" Polarization Curves - APG

B) 37mm Polarization Curves – MM Cued ID 292

Figure 14. Principle polarizability curves for a 37 mm projectile.
The curves on the left (A) represent the average six or eight curve sets extracted from data sets observed over 37 mm projectiles in the Calibration Lanes at APG. The curves on the right were extracted from static data set, SLOStatA00292.tem, the only data set observed over this 37 mm target. This target was missclassified as clutter.

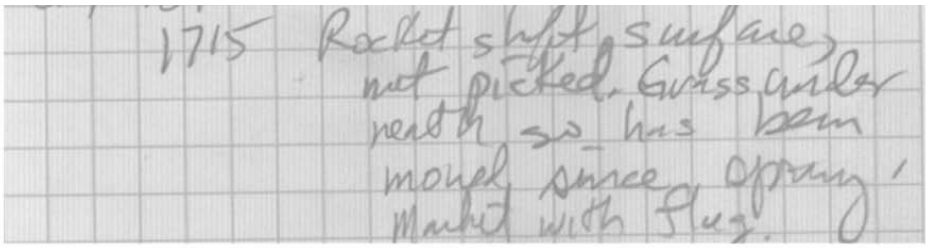

A) Excerpt: Field notes (p. SLO61 6/13/09)

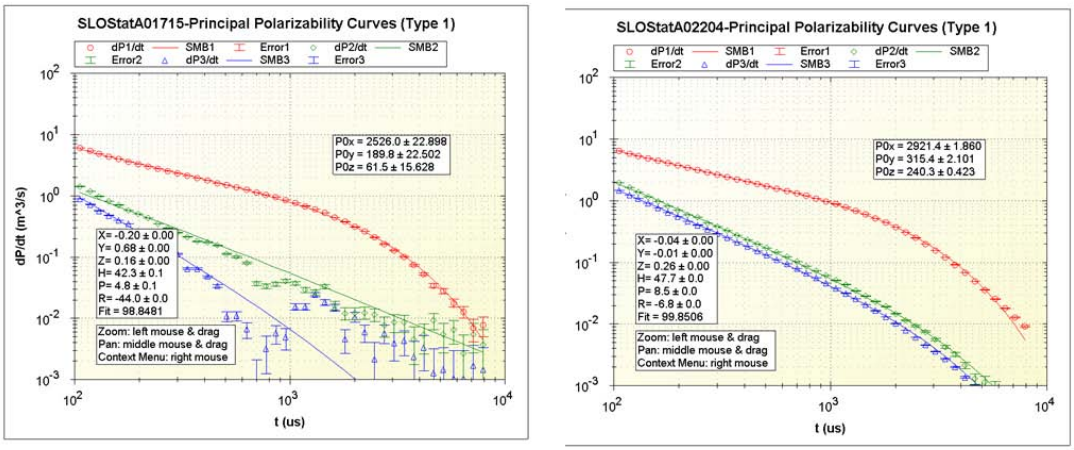

B) C)

Figure 15. Field note describing target near 1715 as a "rocket shaft" (A) together with the polarizability curves for 1715 and a repeat (2204).

The polarizability curves both look like rocket parts. These two data sets are within a meter or two of MM-ID 1718.

8.2.1.2 MM ID 1177/Master ID 775 (60 mm mortar)

The second hard false negative is the 60 mm mortar found in association with MM-ID 1177 (Master List ID 775). The polarizability curves together with the dig photo are in Figure 16.

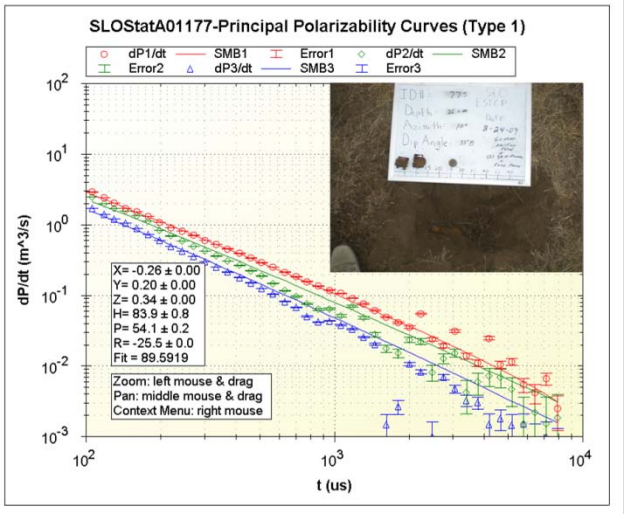

Figure 16. MM cued ID No. 1177 and the corresponding dig photo.

The target in the hole is a 60 mm mortar. The polarizability curves appear to represent the associated tail booms and/or fuse.

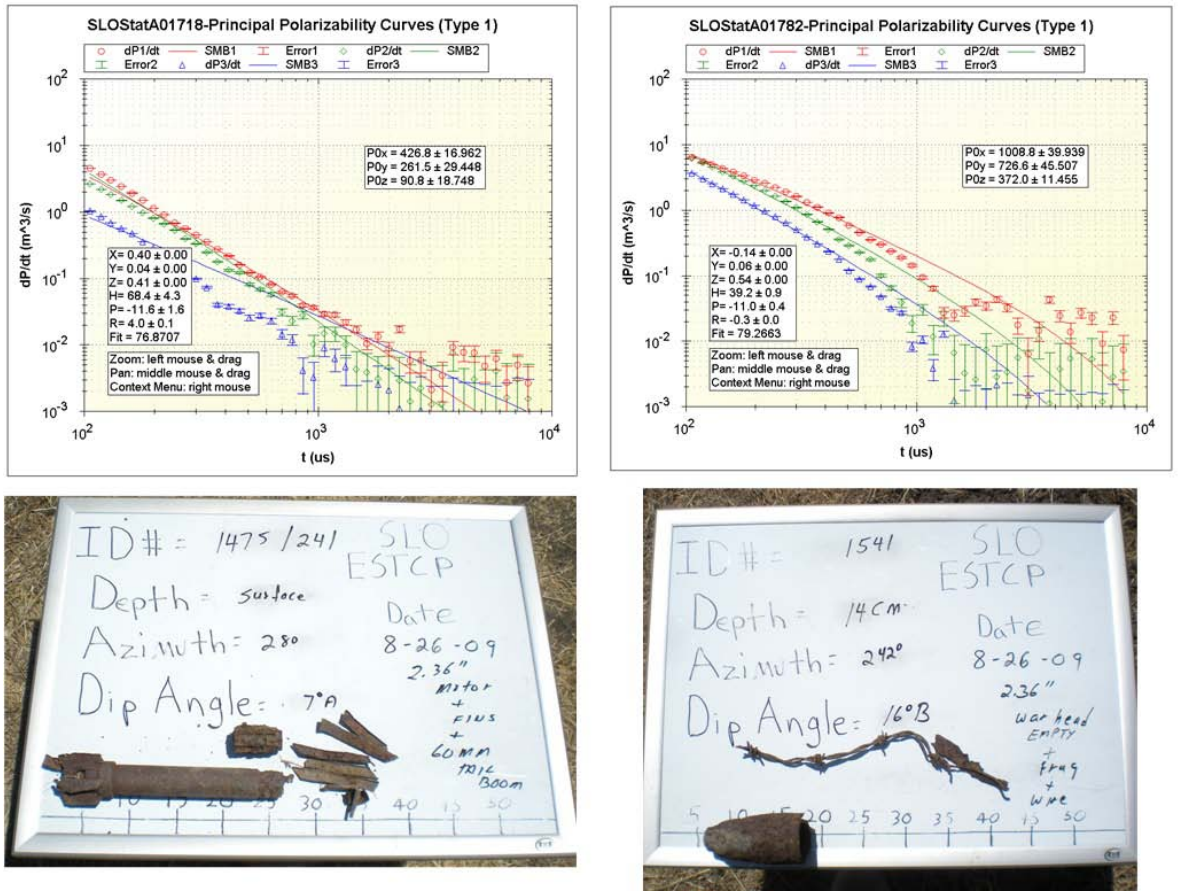

Figure 17. Polarizability curves and dig results for MM-ID Numbers 1718 and 1782, two of four false negatives in both target lists submitted to IDA.

The polarizability curves suggest a shallow equi-dimensional object that is consistent with the 60 mm tail boom segments sitting on the board. The anomaly amplitude is less 10 a microtesla (μT)/s, which means it is only slightly above the detection threshold for a deep mortar. Yet the solution for the target position indicates a target at a depth of 13 cm. It appears therefore that the anomaly produced by the tail boom(s), which no doubt were found above the deep mortar shown in the photo, totally overpowers the low signal level from the mortar. This is a case where the interference from several shallow sources obscures the deeper TOI. The best and only chance we have of mitigating this type of anomaly is to recognize that it is a complex response that cannot be analyzed and therefore must be dug.

8.2.1.3 MM-ID 1718/Master ID 1475 (2.36-inch rocket motor)

The polarizability curves for MM targets 1717 and 1718 and the size estimates indicate that the parameters most likely belong to the 60 mm tail boom shown in the dig photo rather than the rocket motor. The polarizability response of an isolated rocket motor is significantly larger and shows good symmetry and large aspect. This target intrigued us partly because it is a hard false negative but also because the dig reports that the target was found laying on the surface. How then could we have missed a target like that? In looking through our field notes, we came across a note for file SLOStatA01715, a static data point acquired in the immediate vicinity of 1718.

The note (see Figure 15A) indicates that a measurement on an unpicked point was acquired near or over a "rocket shaft" that had obviously been moved recently because it was lying on top of the grass. It is likely that a rocket motor was found in the immediate vicinity (i.e., within a radius of 1 m or so) and lumped in with the 60 mm tail boom. The ground truth indicates the target was found within a distance of 0.3 m of the location of MM 1718. Our theory is that this object was moved after the target detection survey, so this does not represent a failure of our analysis to correctly classify the object.

8.2.1.4 MM-ID 1782/Master ID 1541 (2.36-inch rocket motor)

Relatively speaking, target number MM-ID 1782 (Master ID 1541) is the least important of the four false negative targets that are labeled on both panels of Figure 13. The position of this target is roughly the same on both ROC curves (Figure 13 A & B) and requires only a few unnecessary digs past the operating point (dark blue dot) to get to the target. We mention it here only for completeness. We would like to note, however, that the target (Master ID 1541) is similar in both appearance and in the behavior of its principal polarizability curves to target SLO Master ID 1322 that was belatedly labeled "MD" after a more careful examination. The polarizability curves and photos of MM targets 954 and 1782 provide a comparison between the two targets, one labeled "MD" and the other labeled "TOI." The similar behavior of the polarizability curves suggests that target 1782 is cracked or otherwise physically damaged in a way similar to that of 954. Because this item was so heavily damaged, it no longer exhibits the properties we expect of such a TOI. In fact, this item is so heavily damaged, it barely classifies as a TOI at all.

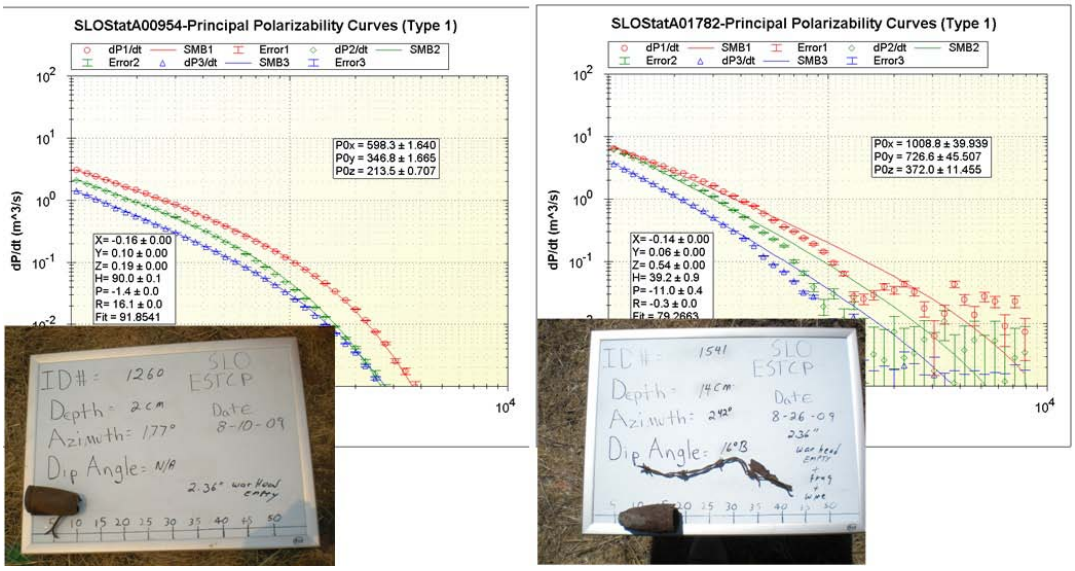

Figure 18. Polarizability curves for two 2.36-inch "empty" warheads.
The target on the left is from the training dig; the one on the right is from the test dig. Although target 1782/1541 was deeper than 954/1260, both targets exhibit similar behavior in the early time.

8.3 MAXIMIZE CORRECT CLASSIFICATION OF CLUTTER

In the test data set, there were a total of 857 clutter objects. The results from ANN 2 (Figures 10B and 13B), show that after ~300 unnecessary digs, we have excavated all the TOIs (Pd = 100%). Therefore, we found all the TOIs after a total of 506 digs and would be able to safely leave the remaining 557 clutter targets in the ground. This represents a reduction of 65% in false alarms and thus we exceed the performance goal of a 30% reduction.

8.4 MINIMIZATION OF "CANNOT ANALYZE" POINTS

Of the 1063 targets that were scored, there were 15 category 4 targets ("cannot analyze"). Those were targets for which the fit statistic was less than 75. The points represent 1.4% of all the targets analyzed. Using the ground truth from the test dig, we determined that the discrimination results for all 15 category data points were correct. Although we do not feel comfortable with completely eliminating a screening rule that relegates data points with poor fit to category 4, in retrospect we think that we were too conservative in assigning the Fit<75% threshold. By assigning a slightly lower threshold (e.g., Fit < 70%), we can eliminate half the category 4 points with little or no danger of introducing a false negative. In any case, MM has clearly met the performance goal of >90% of all targets being analyzable.

8.5 DYNAMIC-MODE SURVEY PRODUCTIVITY

Our performance objective for dynamic-mode survey productivity was 1.2 acres/day. In Table 2, we have tabulated the work time for each of the sub-areas that we defined within the overall demonstration area. These time intervals (Δt) represent the time between the first and last dynamic calibration of the day (or last calibration for a particular sub-area survey) and therefore include time for breaks and breakdowns. What those time intervals do not include is the time for set-up and take-down each day. We estimate that time to be 0.5 hr/day. We based our production estimates on the number of work hours. At SLO, we generally worked about 9-10 hr in the field. Therefore, we converted hourly production to daily production by dividing by 9 hr/day. Based on the table, we met or slightly exceeded our production goal (0.054 ha/hr = 0.49 ha/day = 1.22 acre/day).

The table shows that we have met or exceeded our performance goal for dynamic-mode survey productivity (1.2 acre/day).

Table 2. Dynamic survey productivity at SLO.

		Work Time				Production		File No			Area
Sub-Area	Date	Start	End	Δt	Δt (hr)	Rte (ha/hr)	Rte (ha/d)	1st	Last	Blks	(ha)
NWA	5/25/09	12:33	17:45	5:12	5.20	0.035	0.18	1	47	2	0.18
NWB	5/26/09	7:12	14:51	7:39	7.65	0.035	0.27	48	101	3	0.27
NWC	5/26/09	15:48	17:48	2:00	2.00			102	116		
NWC	5/27/09	7:16	16:14	8:58	8.97	0.046	0.43	117	232	6	0.54
NWC	5/28/09	6:59	7:46	0:47	0.78			233	254		
SWA	5/28/09	9:13	15:41	6:28	6.47	0.042	0.27	255	338	3	0.27
SA	5/29/09	6:59	16:51	9:52	9.87	0.055	0.54	339	424	6	0.54

Table 2. Dynamic survey productivity at SLO (continued).

Sub-Area	Date	Work Time				Production		File No		Blks	Area
		Start	End	Δt	Δt (hr)	Rte (ha/hr)	Rte (ha/d)	1st	Last		(ha)
SE	5/30/09	7:11	12:14	5:03	5.05	0.088	0.54	425	516	9.5	0.855
SE-A	5/30/09	12:52	17:32	4:40	4.67			517	576		
E	5/31/09	6:01	15:59	9:58	9.97	0.068	0.68	577	687	7.5	0.675
NE	6/1/09	7:24	17:13	9:49	9.82	0.057	0.56	688	785	6.2	0.558
NE-A	6/2/09	7:41	12:22	4:41	4.68	0.035	0.16	786	861	1.8	0.162
N	6/9/09	5:42	15:47	10:05	10.08	0.071	0.72	862	1061	8	0.72
NWB-Rep	6/15/09	8:45	11:23	2:38	2.63	0.103	0.27	1062	1105	3	0.27
Totals					**87.83**	**0.054** (avg)	**0.46** (avg)			**56**	**5.04** (avg)

8.6 STATIC-MODE SURVEY PRODUCTIVITY

Our performance goal at SLO was to acquire greater than 200 static data points per day. Table 3 shows that, at SLO, our static productivity was 39 pts/hr. At SLO, we measured 494 pts on our best day.[5] The improved production rates reflect the front-mounted antenna deployment. Secondly, we decreased the stacking time by a factor or 2 because of the generally better signal-to-noise ratio (SNR) at SLO.

Table 3. Static-mode survey productivity at Camp SLO.

Area	Date	Work Time				Production		File Index	
		Start	End	Δt	Δt (hr)	Rte (pts/hr)	Rte (pts/d)	1st	Last
Tst Strip	6/3/09	7:27	8:40	1:13	1.22	17	201	2	22
Tst Pit	6/3/09	9:03	10:18	1:15	1.25	27		23	56
Tst Strip	6/8/09	7:39	8:35	0:56	0.93	13	242	57	68
NWC	6/8/09	9:22	14:25	5:03	5.05	43		1	217
NWC	6/10/09	14:37	17:40	3:03	3.05	41	197	364	489
NWB	6/10/09	8:23	11:48	3:25	3.42	43		218	363
NWA	6/10/09	17:41	18:34	0:53	0.88	40		490	524
NEPlus	6/11/09	8:35	15:21	6:46	6.77	40	405	525	795
E	6/11/09	15:33	18:18	2:45	2.75	57		796	952
E	6/12/09	8:13	13:10	4:57	4.95	51	494	953	1205
SEPlus	6/12/09	14:18	18:08	3:50	3.83	60		1206	1434
Splus	6/13/09	8:30	17:01	8:31	8.52	50	449	1435	1859
N	6/14/09	9:46	17:25	7:39	7.65	42	375	1860	2178
Stat-Rep	6/15/09	12:40	18:42	6:02	6.03	17	155	2179	2282
Stat-Rep	6/16/09	8:47	17:33	8:46	8.77	24	216	2283	2492
Totals					**65.07**	**39** (avg)	**354** (avg)	**2559** (avg)	

[5] At SLO, our access to the site was unrestricted. We generally stayed a full 10 hr at the site. Daily production rates at SLO partly reflect longer work days than at APG. For comparing production rates it is better to use the hourly rates.

9.0 COST ASSESSMENT

9.1 COST MODEL

In Table 4 we provide a cost model for the deployment of the MM technology.

Table 4. Cost model for an MM deployment.

Cost Element	Data Tracked During Demonstration	Estimated Costs
Instrument cost	Component costs and integration costs • Engineering estimates based on current development • Lifetime estimate Track consumables and repairs	$100K-$120K
Mobilization and demobilization	Cost to mobilize to site Derived from demonstration costs	$20K/$15K
Instrument setup costs	Unit: $ cost to set up and calibrate Data Requirements: • 0.5 hr • 2 people • twice per day	$500/day
Survey costs (Dynamic)	Unit: $ cost per hectare Data requirements: • Hours per hectare – 18 hr • Personnel required - 2	$7.2K/ha
Survey costs (Static)	Unit: $ cost per 300 targets Data requirements: • Hours– 9 hr • Personnel required - 2	$3.6K
Detection data processing costs	Unit: $ cost per hectare Data requirements: • Time required – 18 hr • Personnel required - 1	$6.6K
Discrimination data processing costs	Unit: $ per 300 anomaly anomalies • Time required – 9 hr • Personnel required – 1 unit	$3.3K

9.1.1 Equipment Costs

Major subsystems comprising the MM system together with their respective cost estimates are listed in Table 5.

Table 5. Major components comprising a MM system.

MM Component Name	Cost
Antenna platform and DAQ system	$65K
RTK GPS system	$30K
Platform attitude sensor	$5K
Vehicle deployment	$5K-$20K
Software	$10K-$20K

Antenna Platform and DAQ—The antenna platform and the DAQ comprise the proprietary hardware. The platform can be deployed as-is as a human-powered cart. The instrument containing the DAQ can be mounted on a pack-frame and carried by an operator.

RTK GPS System—The location of the antenna platform is normally measured using an RTK GPS system in which the roving antenna is fixed to the antenna platform.

Platform Attitude Sensor—We use an attitude sensing module that contains a two-axis accelerometer to measure pitch and roll angles and a three-axis fluxgate magnetometer that provides reference heading to magnetic north.

Deployment—The MM can be deployed either as a man-powered cart or as a vehicle-towed system. There is a large range of possibilities for tow vehicles and therefore we have provided a cost range for the deployment.

Software—Map data is processed using Geosoft OM software. We supply a set of GXs that permit MM data files to be loaded into a GDB. Target parameters are extracted using Geometrics' proprietary modeling software based on the point dipole model. Results of this target parameterization are placed in a Microsoft Access database.

9.1.2 Mobilization and Demobilization

The cost of mobilization includes the cost of equipment preparation and checkout plus the cost of transportation to the job site. The estimated cost includes labor, transportation, and per diem. Demobilization does not include cost for equipment preparation.

9.1.3 Instrument Setup and Calibration

Instrument setup and calibration procedures require approximately one-half hr at the beginning and at the end of each field day. These procedures include setting up the GPS system, conducting operation checks, and performing static and dynamic calibration surveys.

9.1.4 Dynamic Survey Costs

The cost estimate is based on a crew cost of $3600/day. The estimated areal production is based on survey profiles on 0.75 m offsets. Survey speeds are less than 0.5 m/s. Production rates can be improved by increasing the survey speed. Production of up to 1 ha/day is possible at a survey speed of 1 m/s.

9.1.5 Static Survey Costs

The cost of static surveys is based on an average production rate of 300 static pts/day. At SLO we averaged well over 300 pts/day with the antenna array mounted to the front loader of a Kabota four-wheel drive tractor. Production rates will vary depending on the type of deployment.

9.1.6 Detection Data Processing

A single data analyst can process the data produced by an MM crew. It requires approximately one hour of the analyst's time per hour of field data production. Processing includes loading the data, producing a detection map, and picking targets. It also includes sequencing the target lists for static surveys.

9.1.7 Discrimination Data Processing

As with detection surveys, a competent data analyst is able to keep up with the processing of the data acquired by the MM field crew (~300 static pts/day). Costs are figured accordingly. Note that these costs do not include the costs of training the discrimination algorithm.

9.2 COST DRIVERS

The cost estimates in Table 4 use higher labor costs that reflect the personnel involved in early demonstrations. These labor costs will no doubt drop by as much as one-third as field operations and data processing tasks become routine and are accomplished by lower-level personnel. The productivity of detection surveys is likely to improve by as much as a factor of 2 as we increase survey speed. And finally, the productivity of the data analyst stands to improve markedly as processing tasks are integrated and automated. It is likely that cost of processing will decrease by as much as 50%.

9.3 COST BENEFIT

The cost benefit of employing advanced EMI technology such as the MM can be realized only to the extent that regulators gain sufficient confidence in the technology that they are comfortable letting targets that have been classified "High Confidence Not Munitions" remain undug in the ground. Based on the cost estimates provided in Table 4, the unit cost for cued ID analysis of a target with the MM is approximately $20/target with the costs likely to drop rapidly down to $10/target. The unit cost to dig has been estimated to run between $100-$200/target. The scoring results for the MM showed that fully 98% of the munitions would have been dug with a corresponding false positive dig rate of less than 10% if the targets had been dug according to the prioritized dig list. This suggests that by employing such a dig list in a very conservative manner

at least half of the targets could be left in the ground, thereby reducing the digging costs by half. Since the MM static survey and data analysis costs are approximately 10-20% of the cost to dig, the overall cost of remediation would be reduced by 30-40% (i.e., dig 50% of targets and conduct a cued ID target survey with the MM of 100% of the targets at a cost of 10-20% of the cost to dig).

10.0 IMPLEMENTATION ISSUES

In Section 9, we highlighted the most important issue affecting the implementation of the MM technology. Clearly, the need is to prove to the authorities that regulate and supervise the remediation of sites contaminated with UXO that the MM technology can significantly reduce the cost remediation. We think that the ESTCP PO together with regulators and demonstrators are making some headway with their live site demonstration program. Thus far, successful demonstrations at Camp Siebert, AL; Camp SLO, CA; and Camp Butner, NC, have been completed. The ESTCP PO plans to continue the live site demonstration program, and the MM will be used extensively.

Even with the reduction in the unit survey costs, the cost for deploying the MM will remain significantly higher than the cost for commercially available EMI technology such as the EM61. Clearly, this higher cost is justified provided that regulating authorities accept the discrimination capability of the system and use the results to reduce the number of unnecessary digs. UXO contractors will no doubt begin to deploy advanced EMI systems such as the MM only when regulating authorities start specifying the use of such technology in the big requests relating to UXO site remediation. Clearly, it is important that the MM participated in the demonstration at SLO and performed well. It is equally important that several other data processing demonstrators, using MM data, performed equally as well.

The MM system is available as a commercial product by Geometrics, Inc. It can be deployed in the field using personnel with the same technical skills as those who routinely conduct UXO-related geophysical mapping surveys. In some respects, data processing is more demanding. However, we are confident that this too can be routinely performed by geophysical data processors with a few days training.

This page left blank intentionally.

11.0 REFERENCES

[1] T. Bell, H. Nelson, D. George, J. Kingdon, and D. Keiswetter. 2008. "EMI Array for Cued UXO Discrimination," in *SEG Las Vegas 2008 Annual Meeting*. Las Vegas, NV. pp. 2907-2911.

[2] Defense Science Board. 2003. "Report of the Defense Science Board Task Force on Unexploded Ordnance," U.S. Department of Defense, Washington, DC. November 2003.

[3] R. Loder, G. Robitaille, E. Cespedes, T. Berry, D. Teefy, A. Andrews, M. Chambers, B. Kaschenbach, G. Rowe, J. Moulton, S. Nussbaum, S. Patane, D. Reidy, R. Young, and F. Rotondo. 2002. "Standardized UXO Technology Demonstration Sites Handbook." U.S. Army Environmental Center, Aberdeen Proving Ground, MD. October 2002.

[4] J.S. McClung, "Standardized UXO Technology Demonstration Site Scoring Record No. 921 (Geometrics, Inc)," U.S. Army Aberdeen Test Center, Aberdeen Proving Ground, MD. Final. April 2009.

[5] S. Cazares and M. Tuley. 2009. "UXO Classification Study: Scoring Memorandum for the former Camp San Luis Obispo, CA." Institute for Defense Analyses, Alexandria, VA. Memorandum, March 20, 2009.

[6] Y. Das, J.E. McFee, J. Toews, and G.C. Stuart. 1990. "Analysis of an Electromagnetic Induction Detector for Real-Time Location of Buried Objects." *IEEE Trans. Geosci. & Remote Sensing*, vol. 28, pp. 278-288.

[7] R.E. Grimm. 2003. "Triaxial Modeling and Target Classification of Multichannel, Multicomponent EM Data for UXO Discrimination." *Jour. Envir. & Eng. Geophys*, vol. 8, pp. 239-250.

[8] S. MacInnes, S. Urquhart, and K. Zonge. 2004. "Improving UXO Detection with Four-Dimensionsl Matched Filters." in *Symposium for Applied Geophysics for Environmental and Engineering Problems (SAGEEP) 2004*, Colorado Springs, CO.

[9] H.H. Nelson and J.R. McDonald. 2001. "Multisensor Towed Array Detection System for UXO Detection." *IEEE Trans Geosci & Rem. Sensing*, vol. 39, p. 7, June 2001.

[10] J.T. Smith and H.F. Morrison. 2004. "Estimating Equivalent Dipole Polarizabilities for the Inductive Response of Isolated Conductive Bodies." *IEEE Trans. on Geosc. & Rem. Sens.*, vol. 42, pp. 1208-1214.

[11] L.R. Pasion. 2007. "Inversion of Time Domain Electromagnetic Data for the Detection of Unexploded Ordnance." Ph.D. thesis. Department of Earth and Ocean Sciences, University of British Columbia, Vancouver.

[12] J.T. Smith and H.F. Morrison. 2004. "Estimating Equivalent Dipole Polarizabilities for the Inductive Response of Isolated Conductive Bodies." *IEEE Trans. Geosci. & Rem. Sens.*, vol. 42, pp. 1208-1214.

[13] R.S. Smith and T.J. Jones. 2002. “The moments of the impulse response: A new paradigm for the interpretation of transient electromagnetic data.” *Geophysics*, vol. 67, pp. 1095-1103.

APPENDIX A

POINTS OF CONTACT

Point of Contact	Organization	Phone Fax E-Mail	Role
Mark Prouty	Geometrics, Inc. 2190 Fortune Drive San Jose, CA 95131	Phone: (408) 428-4212 Fax: (408) 954-0902 E-mail: markp@geometrics.com	Principal Investigator
Skip Snyder	Snyder Geoscience 671 Crescent Court Grand Junction, CO 81505	Phone: (970) 254-0330 E-mail: skips@bresnan.net	Co-Principal Investigator
David George	G&G Sciences 873 23rd Road Grand Junction, CO 81505	Phone: (970) 263-9714 E-mail: dgeorge@ggsciences.com	Co-Principal Investigator
ESTCP	ESTCP Program Office 901 N. Stuart Street, Suite 303 Arlington, VA 22203	Phone: (703) 696-2117 Fax: (703) 696-2114	Program Office

ESTCP Office
901 North Stuart Street
Suite 303
Arlington, Virginia 22203

(703) 696-2117 (Phone)
(703) 696-2114 (Fax)

E-mail: estcp@estcp.org
www.serdp-estcp.org